Guest-Induced Phase Switching in a Square Lattice Coordination Network to Enable Selective Adsorption of *p*-Xylene

Shi-Qiang Wang,*[a] Catiúcia R. M. O. Matos,[b] Shaza Darwish,[b] Volodymyr Bon,[c] Yifei Luo,[a] Jun Zhu,[a] Xiaofei Zhang,[a] Zhengtao Xu,[a] Stefan Kaskel,[c] and Michael J. Zaworotko*[b]

[a]Institute of Materials Research and Engineering (IMRE), Agency for Science, Technology and Research (A*STAR), 2 Fusionopolis Way, Singapore 138634, Republic of Singapore.

[b]Bernal Institute and Department of Chemical Sciences, University of Limerick, Limerick V94 T9PX, Republic of Ireland.

[c]Faculty of Chemistry, Technische Universität Dresden, Bergstrasse 66, 01062 Dresden, Germany.

Supporting Information Placeholder

ABSTRACT: Flexible coordination networks featuring guest-induced structural transitions attract increasing attention, as their dynamic pore size/shape adjustments enable exceptional hydrocarbon uptake and selectivity. Herein we studied the self-adaptive phase switching behaviour of the square lattice (**sql**) coordination network $[Cu(4,4'\text{-bipyridine})_2(CF_3CO_2)_2]_n$ (**sql-1-Cu-CF_3CO_2**) upon xylene adsorption. Competitive adsorption studies in binary xylene mixtures revealed PX selectivity of 10.83 over OX and 14.18 over MX, while the overall PX selectivity derived from a ternary mixture reached 10.01, surpassing most commercial zeolites. Crystallographic analysis provided structural insights into the observed PX selectivity, identifying three distinct xylene-loaded phases with varying pore/channel dimensions: 1D for PX (void: 33.9 %), 2D for OX (void: 45.8 %) and 3D for MX (void: 48.4 %). The PX-loaded structure exhibited the smallest void but the strongest host–guest interactions, making it the preferred phase for PX separation from xylene mixtures.

The separation and purification of chemical mixtures using traditional methods such as distillation and crystallization account for 10-15 % of global energy consumption.[1] With the rising demand for commodity chemicals, there is an urgent need for energy-efficient purification technologies. One of the most challenging separations involves xylene isomers: *o*-xylene (OX), *m*-xylene (MX), and *p*-xylene (PX), which are essential for producing fibers, plastics, and fuel additives.[1-3] Among them, PX dominates the xylene market (~ 90 %) due to its extensive use in polyethylene terephthalate production.[4] However, the similar physicochemical properties of xylene isomers make their separation via conventional purification methods highly energy-intensive and inefficient.[1-4] While adsorption-based technologies have been established for xylene separation, their widespread implementation is hindered by the moderate capacity (~ 15 wt%) and selectivity (~ 5) of current adsorbents, i.e. FAU zeolites.[5]

To address this matter, a variety of porous materials has been developed, including molecular materials such as coordination complexes,[6-10] organic molecules and cages,[11-14] as well as extended-dimensional materials like porous coordination polymers/networks (PCPs/PCNs) and metal–organic frameworks (MOFs).[15-34] The latter represent a promising class of metal–organic materials (MOMs),[35,36] offering precise control over pore size, shape, and chemistry through crystal engineering or reticular chemistry,[37,38] with significant potential for hydrocarbon separation.[39-46] To date, a considerable number of rigid MOMs with fixed pore geometries have been investigated for xylene separation.[45,46] However, they typically lack a combination of strong selectivity (> 5) and high adsorption capacity (> 15 wt%). In contrast, flexible MOMs are particularly attractive because they can undergo guest-induced structural transitions, enabling breathing, switching/gate-opening, swelling or induced-fit mechanisms that dynamically adjusts pore size and shape to enhance the adsorption capacity and/or selectivity.[47-54] Nevertheless, flexible MOMs still remain underexplored primarily due to the difficulty in determining their guest-loaded structures,[55,56] which hampers the elucidation of their structural transformations and, consequently, a fundamental understanding of their adsorption mechanisms and structure-property relationships.

Recently, we studied the adsorption properties of a series of square lattice (**sql)** coordination networks (CNs) $[M(bpy)_2(NCS)_2]$, sql-1-M-NCS (1 = bpy =4,4′-bipyridine, M = Fe, Co, and Ni).[57-62] Adsorption isotherms for gases (CO_2, C_2H_x and C_3H_x) and vapors (xylene isomers) exhibited stepped or sigmoidal profiles (denoted as type F-IV).[53] Crystallographic studies elucidated that the interlayer distance in the closed phase (4.5 Å) expanded to 5.4, 6.3, and further to 9.1-9.3 Å in the CO_2-, C_2H_4-, and xylene-loaded phases, respectively.[57-59,62] This adsorbate-dependent phase switching behaviour prompted us to evaluate the xylene separation performance of **sql-1-Co-NCS**, which exhibited a strong preference for OX with a remarkable adsorption capacity of up to 87.5 wt%.[58] Subsequently, by substituting half of the bpy linkers with 4,4′-bis(4-pyridyl)tetrazine (bptz), we synthesized a new rectangular mixed-linker **sql** CN $[Co(bpy)(bptz)(NCS)_2]_n$ (**sql-1,3-Co-NCS**), which exhibited decent xylene adsorption capacity (~ 37 wt%) and high selectivity (> 10) for each xylene isomer over ethylbenzene.[63]

In this contribution, we developed a new analogue of **sql-1-Co-NCS** by substituting the metal cation Co(II) with Cu(II) and replacing the NCS^- counter anion with $CF_3CO_2^-$. We further investigated its xylene separation performance through competitive adsorption experiments in binary and ternary liquid xylene mixtures, analyzed by gas chromatography (GC). Additionally, powder and single-crystal X-ray diffraction (PXRD/SCXRD) studies were conducted to identify the xylene-loaded phases and gain insights into the structural flexibility driven by the host-guest interactions.

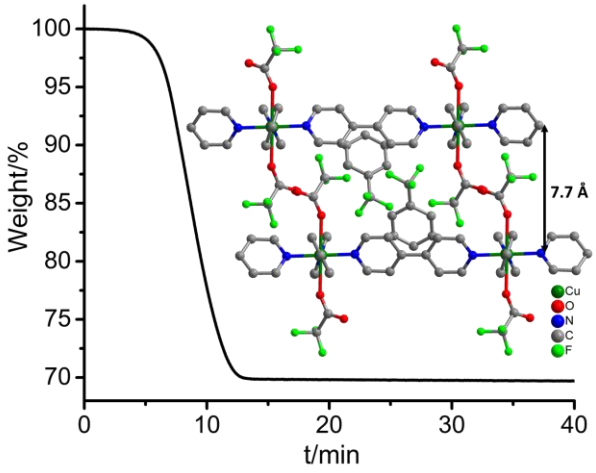

Figure 1. Crystal structure of **sql-1-Cu-CF_3CO_2·2TFT** (H atoms are omitted for clarification), which can be fully activated by heating at 100 °C for 30 min as indicated by the TGA curve.

Single crystals of $\{[Cu(bpy)_2(CF_3CO_2)_2]\cdot 2TFT\}_n$ (**sql-1-Cu-CF_3CO_2·2TFT**, TFT = *α,α,α*-trifluorotoluene) were synthesized via solvent diffusion, following a procedure similar to that used for **sql-1-Co-NCS·2TFT**.[57] Bulk phase purity was confirmed by PXRD (Figure S1). SCXRD analysis (Table S1) revealed that **sql-1-Cu-CF_3CO_2·2TFT** crystallizes in the monoclinic space group *C2/c* (*a*: 22.59 Å, *b*: 11.16 Å, *c*: 16.43 Å, *β*: 112.54°) and maintains the expected **sql** topology, with Cu(II) ions equatorially coordinated by four bpy ligands and axially by two terminal CF_3CO_2 ligands. TFT molecules reside in the interlayer space with an interlayer distance of 7.7 Å (Fig. 1), which is much larger than that of **sql-1-Co-NCS·2TFT** (6.6 Å) due to the bulkier CF_3CO_2 ligands and the more vertical orientation of TFT molecules (Fig. S2a,b). The bpy ligands in **sql-1-Cu-CF_3CO_2·2TFT** adopt two conformations: half coplanar and half twisted (43.5°), closely resembling those in **sql-1-Co-NCS·2TFT** (Fig. S2c,d).[57] The activated phase, **sql-1-Cu-CF_3CO_2**, was isolated by heating **sql-1-Cu-CF_3CO_2·2TFT** at 100 °C for 30 min as confirmed by thermogravimetric analysis (TGA) and variable-temperature PXRD (Figure 1 and S3-S5). Although direct crystal structural determination was unsuccessful, the 77 K N_2 adsorption isotherm indicated that **sql-1-Cu-CF_3CO_2** remained nearly nonporous, with negligible N_2 uptake at low pressure (Fig. S6).

Soaking **sql-1-Cu-CF_3CO_2** in pure OX, MX, and PX separately resulted in the formation of three distinct phases, as revealed by PXRD (Fig. 2a). In contrast, exposure to equimolar binary (PX/MX and PX/OX) or ternary (PX/OX/MX) xylene mixtures led to a single form identical to the PX-soaked phase (Fig. 2a), indicating a strong preference for PX adsorption. To quantify its PX selectivity, the adsorbed xylene molecules were extracted using dichloromethane and the compositions were determined by GC (Fig. 2b). The GC results show prominent PX peaks, with selectivity values of 10.83 and 14.18 for PX over OX and MX, respectively (Fig. S7a,b). The PX selectivity derived from the ternary mixture is 10.01 (Fig. S7c), outperforming most commercial zeolites.[5] These selectivity values are superior or comparable to those of most reported PX-selective adsorbents including $AgLClO_4$,[8] EtP5/6,[11] AZO-cage,[12] P[4]Q[1]L,[14] MIL-125-NH_2,[17] [Ce(HTCPB)],[18] NU-2000,[27] MAF-88,[29] sql-4,5-Zn,[30] polyIRMOF-1-7a,[33] MOF-monoclinic,[64] ZIF-68,[65] Cu(CDC),[66] MIL-140B/MOF-48,[67] DUT-8(Cu),[68] CoPzNi,[69] NIIC-30(Ph),[70] HIAM-201,[71] $[Cu_2Cl_4L_2]$,[72] CAU-1/OH,[73] Zn-ETTOB,[74] and MIL-120(Al),[75] and are surpassed only by a few materials such as Cu-metallocycle,[10] TPBD-αI,[13] MAF-36,[22] ZIF-8/67,[26] Mn-dhbq,[28] MAF-89,[29] HIAM-203,[31] and $Co(aip)(bpy)_{0.5}$.[76]

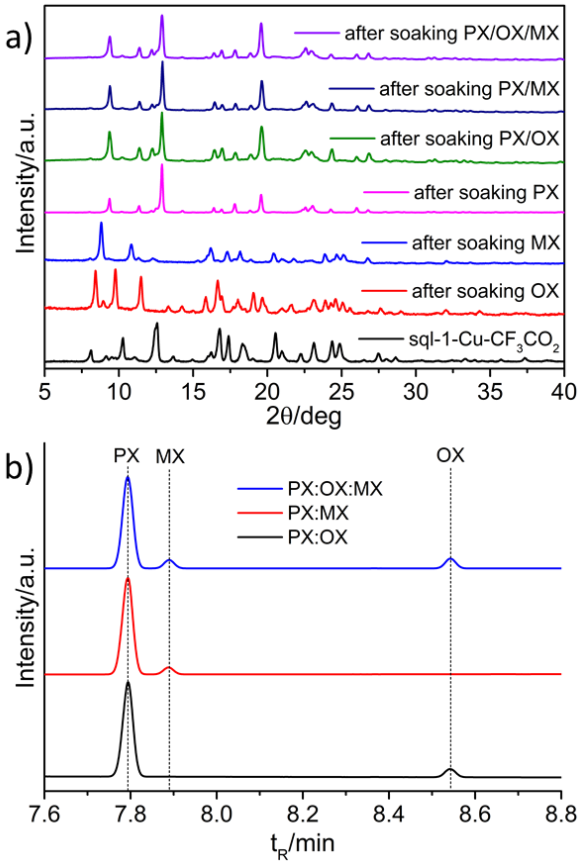

Figure 2. a) PXRD patterns of **sql-1-Cu-CF_3CO_2** before and after soaking in unary, binary and ternary xylene solutions, and b) GC results of the xylene composition extracted from the soaked samples in the binary and ternary xylene mixtures.

To understand the notable PX selectivity of **sql-1-Cu-CF_3CO_2**, single crystals of the xylene-loaded phases were prepared using the same solvent diffusion method, with xylene solvents replacing TFT, and their corresponding crystal structures were successfully determined (Table S1). Although all the xylene-loaded phases adopt the monoclinic space group *C2/c*, their structural characteristics differ significantly. SCXRD analysis revealed that the OX-loaded phase hosts two OX molecules per unit formula (Fig. 3a, denoted as **sql-1-Cu-CF_3CO_2·2OX**), exhibiting unit-cell parameters (*a*: 22.47 Å, *b*: 11.15 Å, *c*: 16.46 Å, *β*: 111.75°) and crystal packing (Fig. 3d) similar to those of **sql-1-Cu-CF_3CO_2·2TFT**, with an identical interlayer distance of 7.7 Å (Fig. 1 and 3a). While the MX-loaded phase also accommodates two MX molecules per unit formula (Fig. 3b, denoted as **sql-1-Cu-CF_3CO_2·2MX**), its unit-cell parameters (*a*: 15.25 Å, *b*: 16.34 Å, *c*: 16.24 Å, *β*: 106.42°) differ from those of **sql-1-Cu-CF_3CO_2·2OX**, and its interlayer distance (7.8 Å) is slightly larger (Fig. 3a,b). Notably, the PX-loaded phase contains only one PX molecule per unit formula (Fig. 3c, denoted as **sql-1-Cu-CF_3CO_2·1PX**), with distinct unit-cell parameters (*a*: 14.27 Å, *b*: 14.45 Å, *c*: 16.95 Å, *β*: 106.99°) compared to the OX and MX-loaded phases. It also features a significantly reduced interlayer distance (6.8 Å), suggesting a stronger host-host/host-guest interactions. In all three xylene-loaded phases, the xylene molecules adopt an ordered and commensurate packing arrangement (Fig. 3d-f and S8), occupying exclusively the interlayer space rather than the square grid cavity, as observed in **sql-1-Co-NCS**.[58] The saturation xylene uptakes of **sql-1-Cu-CF_3CO_2** are 35.2 wt% for OX/MX and 17.6 wt% for PX, comparable to most reported PX-selective adsorbents (Table S2).

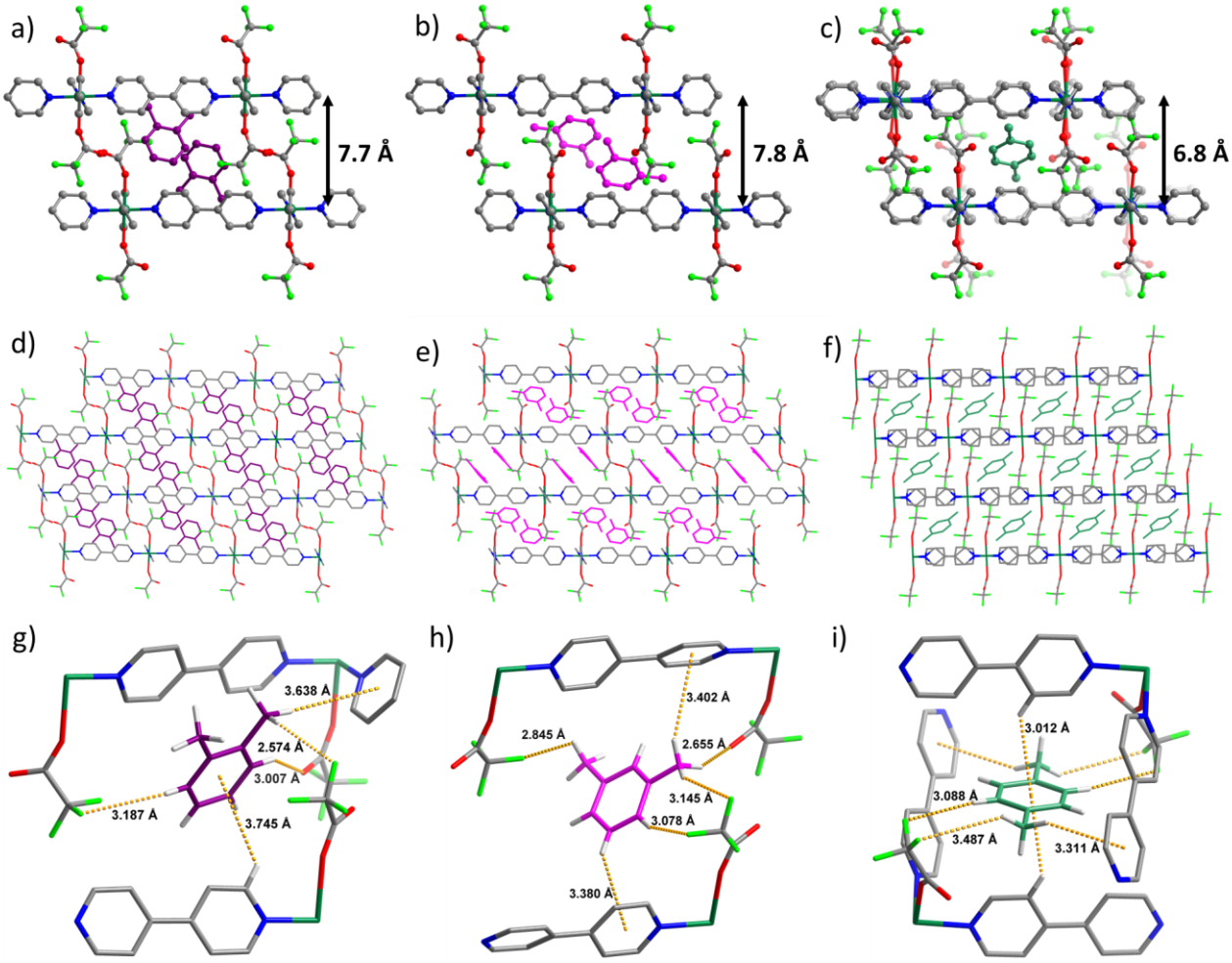

Figure 3. a-c) Crystal structures, d-f) packing arrangements and g-i) host-guest interactions of **sql-1-Cu-CF_3CO_2·2OX**, **sql-1-Cu-CF_3CO_2·2MX,** and **sql-1-Cu-CF_3CO_2·1PX**, respectively. (OX: violet, MX: pink, and PX: sea green.)

Such different structural rearrangements result in distinct host-guest interactions. In the OX-loaded phase (Fig. 3g), two types of C-H···π interactions are present: one between the pyridine hydrogen and the benzene ring of OX (3.745 Å), and another between the methyl hydrogen of OX and the pyridine ring (3.638 Å). Additionally, there are two C-H···F and one C-H···O hydrogen bonds. Two H atoms from the phenyl and methyl groups form two C-H···F hydrogen bonds (3.187 and 2.574 Å) with the F atoms of two CF_3CO_2 groups, while another phenyl H atom forms one C-H···O hydrogen bond (3.007 Å) with the O atom of the CF_3CO_2 group. Similarly, in the MX-loaded phase (Fig. 3h), three C-H···F and one C-H···O hydrogen bonds are observed. A phenyl H atom and two methyl H atoms of the MX contribute to three C-H···F hydrogen bonds (2.845, 3.078, and 3.145 Å), and another methyl H atom forms one C-H···O hydrogen bond (2.655 Å) with the O atom of the CF_3CO_2 group. One phenyl H and one methyl H atom engage in two C-H···π interactions (3.380 and 3.402 Å) with two pyridine rings. Interestingly, in the PX-loaded phase (Fig. 3i), PX establishes symmetric host-guest interactions with the host network. Two methyl H atoms and two phenyl H atoms participate in four symmetric C-H···F hydrogen bonds (3.008 and 3.487 Å). Two additional methyl H atoms form two C-H···π interactions (3.311 Å) with pyridine rings. Furthermore, two H atoms from the pyridine rings contribute to additional C-H···π interactions (3.012 Å) with the phenyl ring of PX. These synergistical noncovalent interactions firmly anchor PX molecules within the pores, explaining why PX is the most strongly adsorbed guest in **sql-1-Cu-CF_3CO_2**.

Due to the self-adaptive structural rearrangements of the host network induced by xylene isomers, the channel voids (probe radius 1.2 Å) of the MX-, OX-, and PX-loaded phases are 48.4, 45.8, to 33.9 % (Fig. 4a-c), respectively. Their channel dimensions also vary (Fig. S9-S11): 3D for the MX-loaded phase, 2D for the OX-loaded phase, and 1D for the PX-loaded phase. In the 2D channel of **sql-1-Cu-CF_3CO_2·2OX**, it is divided into two equal segments due to the staggered packing of the adjacent layers (Fig 4d), which merge into one at the connection zone where the OX molecules reside (Fig. S9). For the 3D channel of **sql-1-Cu-CF_3CO_2·2MX**, it can be simply regraded as 1D, because the channel windows from the other two sides are relatively small (Fig. S10). Indeed, when the probe radius is increased to 2.0 Å, these two small windows disappear, and the channel becomes effectively 1D as similar to that in **sql-1-Cu-CF_3CO_2·1PX** (Fig. S11).The main differences between the channels of MX and PX-loaded phases lie in the orientations of the bpy and CF_3CO_2 ligands. In **sql-1-Cu-CF_3CO_2·2MX**, the pyridine rings of the bpy ligands align parallel to the 1D channel while they penetrate into the 1D channel in **sql-1-Cu-CF_3CO_2·1PX** that reduces the channel void. Furthermore, the CF_3CO_2 ligands protrude into the channel from two opposite sides that further constrict the void, thereby allowing only one PX molecule to be accommodated per unit formula. The smallest void in the PX-loaded structure suggests that it requires the least energy input for the structural rearrangement, therefore making **sql-1-Cu-CF_3CO_2·1PX** the preferred phase for xylene mixture adsorption.

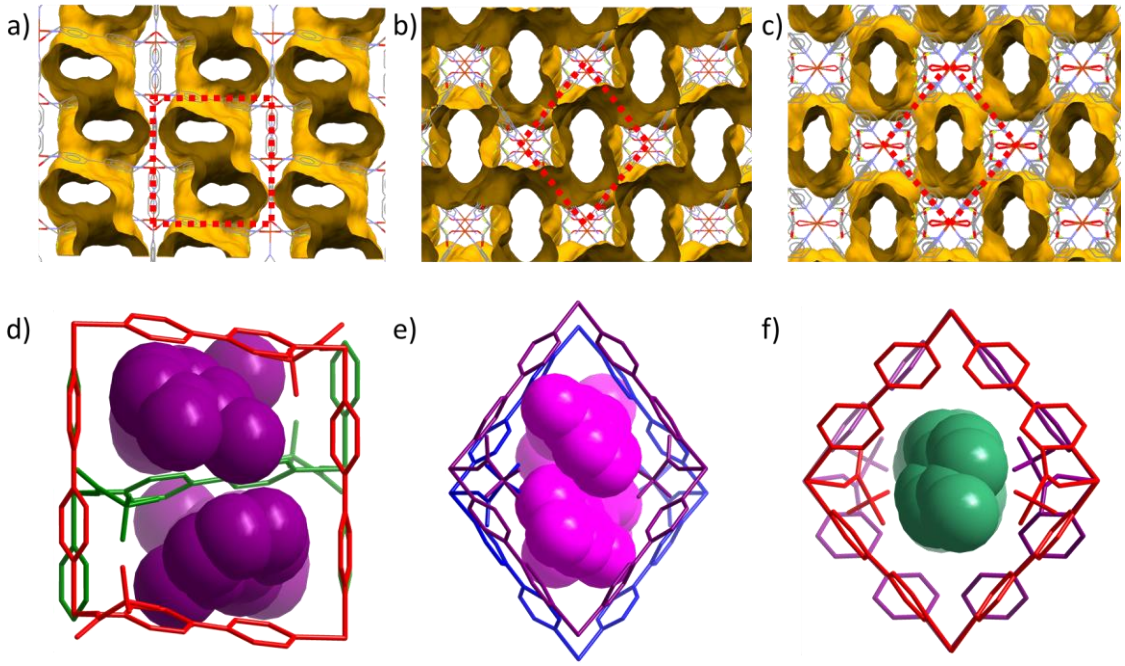

Figure 4. The channel profiles (a-c) and the corresponding enlarged view (d-e) of the red dash line regions for **sql-1-Cu-CF_3CO_2·2OX**, **sql-1-Cu-CF_3CO_2·2MX,** and **sql-1-Cu-CF_3CO_2·1PX**, respectively.

Although it is not uncommon that flexible MOMs exhibit varying saturation uptakes for adsorbates with different sizes, the pore or channel dimensions of the guest-loaded phases typically remain unchanged, as exemplified by the MIL-53 family.[16] In contrast, the xylene-induced structural changes in **sql-1-Cu-CF_3CO_2** are unusual, leading to different unit-cell parameters and host-guest ratio (1:1 for PX and 1:2 for OX/MX), along with three distinct pore/channel dimensions ranging from 1D to 3D. This behavior also differs from that of **sql-1-Co-NCS**,[58] where the host-guest ratio remains 1:4 for all three xylene isomers, despite variations in unit-cell parameters. These differences arise from the flexibility imparted by the clay-like nature of the 2D layered structure, which is held by noncovalent interactions. In addition, **sql-1-Co-NCS** exhibits OX-selective, whereas **sql-1-Cu-CF_3CO_2** is PX-selective. These findings highlight the adaptability of the 2D switching coordination networks.

In conclusion, we investigated the self-adaptive phase switching behaviour of **sql-1-Cu-CF_3CO_2** through xylene adsorption studies under equilibrium conditions. While flexible MOMs have been investigated for their guest-induced structural changes, the emergence of distinct pore profiles in 2D switching CNs induced by xylene isomers remains rare. Crystallographic studies reveal that the choice of metal center and counter anion strongly influences the selective preference of flexible MOMs. Combined with PX selectivity exceeding 10 and PX uptake of 17.6 %, **sql-1-Cu-CF_3CO_2** demonstrates promising separation performance compared to zeolites and other types of adsorbents. To our knowledge, this is only the second example of a 2D MOM exhibiting PX selectivity, following **sql-4,5-Zn**.[30] However, there is still room for improvement in xylene uptake, as **sql-1-Co-NCS** has been shown to adsorb over 85 wt% of xylenes.[58] Further investigations will focus on exploring the adsorption behavior of other aromatic hydrocarbons in these 2D switching layered materials.

AUTHOR INFORMATION

Corresponding Author

E-mail:* wangsq@imre.a-star.edu.sg; xtal@ul.ie

ACKNOWLEDGMENT

M. J. Z. would like to acknowledge the support of Irish Research Council (IRCLA/2019/167) and Science Foundation Ireland (13/RP/B2549 and 16/IA/4624). Z. X. and Y. L. acknowledge the support from the Agency for Science, Technology and Research (SC25/22-119116 and M23L8b0049).

REFERENCES

(1) Sholl, D. S.; Lively, R. P., Seven chemical separations to change the world. *Nature* **2016,** *532* (7600), 435-437.

(2) Fabri, J.; Graeser, U.; Simo, T. A., Xylenes. In *Ullmann's Encyclopedia of Industrial Chemistry*, Wiley-VCH, Weinheim, **2000**.

(3) Cannella, W. J., Xylenes and Ethylbenzene. In *Kirk-Othmer Encyclopedia of Chemical Technology*, Wiley, Hoboken, **2000**.

(4) Mortier, J., *Industrial Arene Chemistry: Markets, Technologies, Sustainable Processes and Cases Studies of Aromatic Commodities,* John Wiley & Sons: **2023**.

(5) Yang, Y.; Bai, P.; Guo, X., Separation of Xylene Isomers: A Review of Recent Advances in Materials. *Ind. Eng. Chem. Res.* **2017,** *56* (50), 14725-14753.

(6) Schaeffer, W. D.; Dorsey, W. S.; Skinner, D. A.; Christian, C. G., Separation of Xylenes, Cymenes, Methylnaphthalenes and Other Isomers by Clathration with Inorganic Complexes. *J. Am. Chem. Soc.* **1957,** *79* (22), 5870-5876.

(7) Lusi, M.; Barbour, L. J., Solid-Vapor Sorption of Xylenes: Prioritized Selectivity as a Means of Separating All Three Isomers Using a Single Substrate. *Angew. Chem., Int. Ed.* **2012,** *51* (16), 3928-3931.

(8) Sun, N.; Wang, S.-Q.; Zou, R.; Cui, W.-G.; Zhang, A.; Zhang, T.; Li, Q.; Zhuang, Z.-Z.; Zhang, Y.-H.; Xu, J.; Zaworotko, M. J.; Bu, X.-H., Benchmark selectivity p-xylene separation by a non-porous molecular solid through liquid or vapor extraction. *Chem. Sci.* **2019,** *10* (38), 8850-8854.

(9) Kałuża, A. M.; Mukherjee, S.; Wang, S.-Q.; O'Hearn, D. J.; Zaworotko, M. J., [Cu(4-phenylpyridine)$_4$(trifluoromethanesulfonate)$_2$], a Werner complex that exhibits high selectivity for o-xylene. *Chem. Commun.* **2020,** *56* (13), 1940-1943.

(10) du Plessis, M.; Nikolayenko, V. I.; Barbour, L. J., Record-Setting Selectivity for p-Xylene by an Intrinsically Porous Zero-Dimensional Metallocycle. *J. Am. Chem. Soc.* **2020,** *142* (10), 4529-4533.
(11) Jie, K.; Liu, M.; Zhou, Y.; Little, M. A.; Pulido, A.; Chong, S. Y.; Stephenson, A.; Hughes, A. R.; Sakakibara, F.; Ogoshi, T.; Blanc, F.; Day, G. M.; Huang, F.; Cooper, A. I., Near-Ideal Xylene Selectivity in Adaptive Molecular Pillar[n]arene Crystals. *J. Am. Chem. Soc.* **2018,** *140* (22), 6921-6930.
(12) Moosa, B.; Alimi, L. O.; Shkurenko, A.; Fakim, A.; Bhatt, P. M.; Zhang, G.; Eddaoudi, M.; Khashab, N. M., A Polymorphic Azobenzene Cage for Energy-Efficient and Highly Selective p-Xylene Separation. *Angew. Chem., Int. Ed.* **2020,** *59* (48), 21367-21371.
(13) Rahmani, M.; Matos, C. R. M. O.; Wang, S.-Q.; Bezrukov, A. A.; Eaby, A. C.; Sensharma, D.; Hjiej-Andaloussi, Y.; Vandichel, M.; Zaworotko, M. J., Highly Selective p-Xylene Separation from Mixtures of C8 Aromatics by a Nonporous Molecular Apohost. *J. Am. Chem. Soc.* **2023,** *145* (50), 27316-27324.
(14) Zhang, G.; Zhang, K.; Lou, X. Y.; Li, X.; Song, C. L.; Huan, W. W.; Yang, Y. W., Separation of p-Xylene from C8 Alkylaromatics by Nonporous Adaptive Crystals of Leggero Pillar[4]arene[1]quinone. *ACS Materials Lett.* **2023,** *6* (2), 446-451.
(15) Alaerts, L.; Kirshhock, C. E. A.; Maes, M.; van der Veen, M. A.; Finsy, V.; Depla, A.; Martens, J. A.; Baron, G. V.; Jacobs, P. A.; Denayer, J. F. M.; De Vos, D. E., Selective adsorption and separation of xylene isomers and ethylbenzene with the microporous vanadium(IV) terephthalate MIL-47. *Angew. Chem., Int. Ed.* **2007,** *46* (23), 4293-4297.
(16) Alaerts, L.; Maes, M.; Giebeler, L.; Jacobs, P. A.; Martens, J. A.; Denayer, J. F. M.; Kirschhock, C. E. A.; De Vos, D. E., Selective Adsorption and Separation of ortho-Substituted Alkylaromatics with the Microporous Aluminum Terephthalate MIL-53. *J. Am. Chem. Soc.* **2008,** *130* (43), 14170-14178.
(17) Vermoortele, F.; Maes, M.; Moghadam, P. Z.; Lennox, M. J.; Ragon, F.; Boulhout, M.; Biswas, S.; Laurier, K. G. M.; Beurroies, I.; Deboyel, R.; Roeffaers, M.; Stock, N.; Duren, T.; Serre, C.; De Vos, D. E., p-Xylene-Selective Metal-Organic Frameworks: A Case of Topology-Directed Selectivity. *J. Am. Chem. Soc.* **2011,** *133* (46), 18526-18529.
(18) E.; Perkins, C. G.; Jelfs, K. E.; Boldrin, P.; Chater, P. A.; Miller, G. J.; Manning, T. D.; Briggs, M. E.; Stylianou, K. C.; Claridge, J. B.; Rosseinsky, M. J., Shape Selectivity by Guest-Driven Restructuring of a Porous Material. *Angew. Chem., Int. Ed.* **2014,** *53* (18), 4592-4596.
(19) Torres-Knoop, A.; Krishna, R.; Dubbeldam, D., Separating Xylene Isomers by Commensurate Stacking of p-Xylene within Channels of MAF-X8. *Angew. Chem., Int. Ed.* **2014,** *53* (30), 7774-7778.
(20) Holcroft, J. M.; Hartlieb, K. J.; Moghadam, P. Z.; Bell, J. G.; Barin, G.; Ferris, D. P.; Bloch, E. D.; Algaradah, M. M.; Nassar, M. S.; Botros, Y. Y.; Thomas, K. M.; Long, J. R.; Snurr, R. Q.; Stoddart, J. F., Carbohydrate-Mediated Purification of Petrochemicals. *J. Am. Chem. Soc.* **2015,** *137* (17), 5706-5719.
(21) Gonzalez, M. I.; Kapelewski, M. T.; Bloch, E. D.; Milner, P. J.; Reed, D. A.; Hudson, M. R.; Mason, J. A.; Barin, G.; Brown, C. M.; Long, J. R., Separation of Xylene Isomers through Multiple Metal Site Interactions in Metal-Organic Frameworks. *J. Am. Chem. Soc.* **2018,** *140* (9), 3412-3422.
(22) Yang, X.; Zhou, H.-L.; He, C.-T.; Mo, Z.-W.; Ye, J.-W.; Chen, X.-M.; Zhang, J.-P., Flexibility of Metal-Organic Framework Tunable by Crystal Size at the Micrometer to Submillimeter Scale for Efficient Xylene Isomer Separation. *Research* **2019,** *2019*, 9463719.
(23) Kim, S.-I.; Lee, S.; Chung, Y. G.; Bae, Y.-S., Origin of p-xylene selectivity in a DABCO pillar-layered metal-organic framework: Combined experimental and computational investigation. *ACS Appl. Mater. Interfaces* **2019,** *11* (34), 31227-31236.
(24) Cui, X.; Niu, Z.; Shan, C.; Yang, L.; Hu, J.; Wang, Q.; Lan, P. C.; Li, Y.; Wojtas, L.; Ma, S.; Xing, H., Efficient separation of xylene isomers by a guest-responsive metal–organic framework with rotational anionic sites. *Nat. Commun.* **2020,** *11* (1), 5456.
(25) Li, X.; Wang, J.; Bai, N.; Zhang, X.; Han, X.; da Silva, I.; Morris, C. G.; Xu, S.; Wilary, D. M.; Sun, Y.; Cheng, Y.; Murray, C. A.; Tang, C. C.; Frogley, M. D.; Cinque, G.; Lowe, T.; Zhang, H.; Ramirez-Cuesta, A. J.; Thomas, K. M.; Bolton, L. W.; Yang, S.; Schröder, M., Refinement of pore size at subangstrom precision in robust metal–organic frameworks for separation of xylenes. *Nat. Commun.* **2020,** *11* (1), 4280.
(26) Polyukhov, D. M.; Poryvaev, A. S.; Sukhikh, A. S.; Gromilov, S. A.; Fedin, M. V., Fine-Tuning Window Apertures in ZIF-8/67 Frameworks by Metal Ions and Temperature for High-Efficiency Molecular Sieving of Xylenes. *ACS Appl. Mater. Interfaces* **2021,** *13* (34), 40830-40836.
(27) Idrees, K. B.; Li, Z.; Xie, H.; Kirlikovali, K. O.; Kazem-Rostami, M.; Wang, X.; Wang, X.; Tai, T.-Y.; Islamoglu, T.; Stoddart, J. F.; Snurr, R. Q.; Farha, O. K., Separation of Aromatic Hydrocarbons in Porous Materials. *J. Am. Chem. Soc.* **2022,** *144* (27), 12212-12218.
(28) Li, L.; Guo, L.; Olson, D. H.; Xian, S.; Zhang, Z.; Yang, Q.; Wu, K.; Yang, Y.; Bao, Z.; Ren, Q.; Li, J., Discrimination of xylene isomers in a stacked coordination polymer. *Science* **2022,** *377* (6603), 335-339.
(29) Ye, Z.-M.; Zhang, X.-F.; Liu, D.-X.; Xu, Y.-T.; Wang, C.; Zheng, K.; Zhou, D.-D.; He, C.-T.; Zhang, J.-P., A gating ultramicroporous metal-organic framework showing high adsorption selectivity, capacity and rate for xylene separation. *Sci. China Chem.* **2022,** *65* (8), 1552-1558.
(30) Gao, M.-Y.; Wang, S.-Q.; Bezrukov, A. A.; Darwish, S.; Song, B.-Q.; Deng, C.; Matos, C. R. M. O.; Liu, L.; Tang, B.; Dai, S.; Yang, S.; Zaworotko, M. J., Switching Adsorbent Layered Material that Enables Stepwise Capture of C8 Aromatics via Single-Crystal-to-Single-Crystal Transformations. *Chem. Mater.* **2023,** *35* (23), 10001-10008.
(31) Yu, L.; Zhang, J.; Ullah, S.; Yao, J.; Luo, H.; Huang, J.; Xia, Q.; Thonhauser, T.; Li, J.; Wang, H., Separating Xylene Isomers with a Calcium Metal-Organic Framework. *Angew. Chem., Int. Ed.* **2023,** *62* (41), e202310672.
(32) Wang, Q.; Li, Y.; Qiu, Z.; Zhou, D.; Yang, L.; Suo, X.; Cui, X.; Xing, H., Highly Efficient Separation of Intermediate-Size m-Xylene from Xylenes via a Length-Matched Metal-Organic Framework with Optimal Oxygen Sites Distribution. *Angew. Chem., Int. Ed.* **2024,** *63* (46), e202408817.
(33) Hyun, T.; Park, J.; So, J.; Kim, J.; Koh, D. Y., Unexpected Molecular Sieving of Xylene Isomer Using Tethered Ligand in Polymer-Metal-Organic Frameworks (polyMOFs). *Adv Sci* **2024,** *11* (34), e2402980.
(34) Xie, X.-J.; Zeng, H.; Huang, Y.-L.; Wang, Y.; Cao, Q.-Y.; Lu, W.; Li, D., Direct production of o-xylene from six-component BTEXs using a channel-pore interconnected metal-organic framework. *Chem* **2024**.
(35) Perry IV, J. J.; Perman, J. A.; Zaworotko, M. J., Design and synthesis of metal–organic frameworks using metal–organic polyhedra as supermolecular building blocks. *Chem. Soc. Rev.* **2009,** *38* (5), 1400-1417.
(36) Cook, T. R.; Zheng, Y.-R.; Stang, P. J., Metal-Organic Frameworks and Self-Assembled Supramolecular Coordination Complexes: Comparing and Contrasting the Design, Synthesis, and Functionality of Metal-Organic Materials. *Chem. Rev.* **2013,** *113* (1), 734-777.
(37) Moulton, B.; Zaworotko, M. J. From Molecules to Crystal Engineering: Supramolecular Isomerism and Polymorphism in Network Solids. *Chem. Rev.* **2001,** *101*, 1629-1658
(38) Ockwig, N. W.; Delgado-Friedrichs, O.; O'Keeffe, M.; Yaghi, O. M. Reticular Chemistry: Occurrence and Taxonomy of Nets and Grammar for the Design of Frameworks. *Acc. Chem. Res.* **2005,** *38*, 176-182.
(39) Wu, H.; Gong, Q.; Olson, D. H.; Li, J., Commensurate Adsorption of Hydrocarbons and Alcohols in Microporous Metal Organic Frameworks. *Chem. Rev.* **2012,** *112* (2), 836-868.
(40) Li, J.-R.; Sculley, J.; Zhou, H.-C., Metal–Organic Frameworks for Separations. *Chem. Rev.* **2012,** *112* (2), 869-932.
(41) Van de Voorde, B.; Bueken, B.; Denayer, J.; De Vos, D., Adsorptive separation on metal–organic frameworks in the liquid phase. *Chem. Soc. Rev.* **2014,** *43* (16), 5766-5788.
(42) Bao, Z.; Chang, G.; Xing, H.; Krishna, R.; Ren, Q.; Chen, B., Potential of microporous metal-organic frameworks for separa-

tion of hydrocarbon mixtures. *Energy Environ. Sci.* **2016,** *9* (12), 3612-3641.

(43) Mukherjee, S.; Desai, A. V.; Ghosh, S. K., Potential of metal–organic frameworks for adsorptive separation of industrially and environmentally relevant liquid mixtures. *Coord. Chem. Rev.* **2018,** *367*, 82-126.

(44) Zhang, Z.; Peh, S. B.; Kang, C.; Chai, K.; Zhao, D., Metal-organic frameworks for C6–C8 hydrocarbon separations. *EnergyChem* **2021,** *3* (4), 100057.

(45) Liu, Y.; Wang, C.; Yang, Q.; Ren, Q.; Bao, Z., Separation of xylene isomers using metal-organic frameworks: Addressing challenges in the petrochemical industry. *Coord. Chem. Rev.* **2025,** *523*, 216229.

(46) Xu, M.; Tang, W.-Q.; Meng, S.-S.; Gu, Z.-Y., Metal–organic frameworks for the separation of xylene isomers. *Chem. Soc. Rev.* **2025,** *54* (3), 1613-1633.

(47) Horike, S.; Shimomura, S.; Kitagawa, S., Soft porous crystals. *Nat. Chem*. **2009**, 1 (9), 695-704.

(48) Schneemann, A.; Bon, V.; Schwedler, I.; Senkovska, I.; Kaskel, S.; Fischer, R. A., Flexible metal-organic frameworks. *Chem. Soc. Rev*. **2014**, 43 (16), 6062-6096.

(49) Chang, Z.; Yang, D.-H.; Xu, J.; Hu, T.-L.; Bu, X.-H., Flexible Metal-Organic Frameworks: Recent Advances and Potential Applications. *Adv. Mater.* **2015,** *27* (36), 5432-5441.

(50) Zhang, J.-P.; Zhou, H.-L.; Zhou, D.-D.; Liao, P.-Q.; Chen, X.-M., Controlling flexibility of metal–organic frameworks. *Natl. Sci. Rev.* **2018,** *5* (6), 907-919.

(51) Elsaidi, S. K.; Mohamed, M. H.; Banerjee, D.; Thallapally, P. K., Flexibility in Metal-Organic Frameworks: A fundamental understanding. *Coord. Chem. Rev.* **2018,** *358*, 125-152.

(52) Krause, S.; Hosono, N.; Kitagawa, S., Chemistry of Soft Porous Crystals: Structural Dynamics and Gas Adsorption Properties. *Angew. Chem., Int. Ed.* **2020,** *59* (36), 15325-15341.

(53) Wang, S.-Q.; Mukherjee, S.; Zaworotko, M. J., Spiers Memorial Lecture: Coordination Networks that Switch between Nonporous and Porous Structures: An Emerging Class of Soft Porous Crystals. *Faraday Discuss.*, **2021**, *231*, 9-50.

(54) Senkovska, I.; Bon, V.; Abylgazina, L.; Mendt, M.; Berger, J.; Kieslich, G.; Petkov, P.; Luiz Fiorio, J.; Joswig, J.-O.; Heine, T.; Schaper, L.; Bachetzky, C.; Schmid, R.; Fischer, R. A.; Pöppl, A.; Brunner, E.; Kaskel, S., Understanding MOF Flexibility: An Analysis Focused on Pillared Layer MOFs as a Model System. *Angew. Chem., Int. Ed.* **2023,** *62* (33), e202218076.

(55) Zhang, J.-P.; Liao, P.-Q.; Zhou, H.-L.; Lin, R.-B.; Chen, X.-M., Single-crystal X-ray diffraction studies on structural transformations of porous coordination polymers. *Chem. Soc. Rev.* **2014,** *43* (16), 5789-5814.

(56) Bon, V.; Brunner, E.; Pöppl, A.; Kaskel, S., Unraveling Structure and Dynamics in Porous Frameworks via Advanced In Situ Characterization Techniques. *Adv. Funct. Mater.* **2020,** *30* (41), 1907847.

(57) Wang, S.-Q.; Yang, Q.-Y.; Mukherjee, S.; O'Nolan, D.; Patyk-Kazmierczak, E.; Chen, K.-J.; Shivanna, M.; Murray, C.; Tang, C. C.; Zaworotko, M. J., Recyclable switching between nonporous and porous phases of a square lattice (sql) topology coordination network. *Chem. Commun.* **2018,** *54* (51), 7042-7045.

(58) Wang, S.-Q.; Mukherjee, S.; Patyk-Kaźmierczak, E.; Darwish, S.; Bajpai, A.; Yang, Q.-Y.; Zaworotko, M. J., Highly Selective, High-Capacity Separation of o-Xylene from C8 Aromatics by a Switching Adsorbent Layered Material. *Angew. Chem. Int. Ed.* **2019,** *58* (20), 6630-6634.

(59) Wang, S.-Q.; Darwish, S.; Sensharma, D.; Zaworotko, M. J., Tuning the switching pressure in square lattice coordination networks by metal cation substitution. *Mater. Adv.* **2022,** *3* (2), 1240-1247.

(60) Wang, S.-Q.; Darwish, S.; Meng, X.-Q.; Chang, Z.; Bu, X.-H.; Zaworotko, M. J., Acetylene storage performance of $[Ni(4,4'\text{-bipyridine})_2(NCS)_2]_n$, a switching square lattice coordination network. *Chem. Commun.* **2022,** *58* (10), 1534-1537.

(61) Wang, S.-Q.; Darwish, S.; Zaworotko, M. J., Adsorbate-dependent phase switching in the square lattice topology coordination network $[Ni(4,4'\text{-bipyridine})_2(NCS)_2]_n$. *Chem. Commun.* **2023,** *59* (5), 559-562.

(62) Wang, S.-Q.; Bon, V.; Darwish, S.; Wang, S.-M.; Yang, Q.-Y.; Xu, Z.; Kaskel, S.; Zaworotko, M. J., Insight into the Gas-Induced Phase Transformations in a 2D Switching Coordination Network via Coincident Gas Sorption and In Situ PXRD. *ACS Materials Lett.* **2024,** *6* (2), 666-673.

(63) Kumar, N.; Wang, S.-Q.; Mukherjee, S.; Bezrukov, A. A.; Patyk-Kaźmierczak, E.; O'Nolan, D.; Kumar, A.; Yu, M.-H.; Chang, Z.; Bu, X.-H.; Zaworotko, M. J., Crystal engineering of a rectangular sql coordination network to enable xylenes selectivity over ethylbenzene. *Chem. Sci.* **2020,** *11* (26), 6889-6895.

(64) Gu, Z.-Y.; Jiang, D.-Q.; Wang, H.-F.; Cui, X.-Y.; Yan, X.-P., Adsorption and separation of xylene isomers and ethylbenzene on two Zn-terephthalate metal-organic frameworks. *J. Phys. Chem. C* **2010,** *114* (1), 311-316.

(65) Van der Perre, S.; Van Assche, T.; Bozbiyik, B.; Lannoeye, J.; De Vos, D. E.; Baron, G. V.; Denayer, J. F. M., Adsorptive Characterization of the ZIF-68 Metal-Organic Framework: A Complex Structure with Amphiphilic Properties. *Langmuir* **2014,** *30* (28), 8416-8424.

(66) Lannoeye, J.; Van de Voorde, B.; Bozbiyik, B.; Reinsch, H.; Denayer, J.; De Vos, D., An aliphatic copper metal-organic framework as versatile shape selective adsorbent in liquid phase separations. *Micropor. Mesopor. Mater.* **2016,** *226*, 292-298.

(67) Gee, J. A.; Zhang, K.; Bhattacharyya, S.; Bentley, J.; Rungta, M.; Abichandani, J. S.; Sholl, D. S.; Nair, S., Computational Identification and Experimental Evaluation of Metal-Organic Frameworks for Xylene Enrichment. *J. Phys. Chem. C* **2016,** *120* (22), 12075-12082.

(68) Kim, S.-I.; Lee, S.; Chung, Y. G.; Bae, Y.-S., Origin of p-xylene selectivity in a DABCO pillar-layered metal-organic framework: Combined experimental and computational investigation. *ACS Appl. Mater. Interfaces* **2019,** *11* (34), 31227-31236.

(69) Shivanna, M.; Otake, K.-i.; Zheng, J.-J.; Sakaki, S.; Kitagawa, S., Control of local flexibility towards p-xylene sieving in Hofmann-type porous coordination polymers. *Chem. Commun.* **2020,** *56* (67), 9632-9635.

(70) Sapianik, A. A.; Dudko, E. R.; Kovalenko, K. A.; Barsukova, M. O.; Samsonenko, D. G.; Dybtsev, D. N.; Fedin, V. P., Metal-Organic Frameworks for Highly Selective Separation of Xylene Isomers and Single-Crystal X-ray Study of Aromatic Guest-Host Inclusion Compounds. *ACS Appl. Mater. Interfaces* **2021,** *13* (12), 14768-14777.

(71) Lin, Y.; Zhang, J.; Pandey, H.; Dong, X.; Gong, Q.; Wang, H.; Yu, L.; Zhou, K.; Yu, W.; Huang, X.; Thonhauser, T.; Han, Y.; Li, J., Efficient separation of xylene isomers by using a robust calcium-based metal–organic framework through a synergetic thermodynamically and kinetically controlled mechanism. *J. Mater.Chem. A* **2021,** *9* (46), 26202-26207.

(72) Ye, J.; du Plessis, M.; Loots, L.; van Wyk, L. M.; Barbour, L. J., Solid–Liquid Separation of Xylene Isomers Using a Cu-Based Metallocycle. *Cryst. Growth Des.* **2022,** *22* (4), 2654-2661.

(73) Chen, K.; Liu, P.; Wang, Y.; Ren, Y.; Li, J.; Chen, Y.; Li, J.; Li, L., Structural functionalization in robust metal–organic frameworks for p-xylene separation with superior adsorption capacity. *Micropor. Mesopor. Mater.* **2023,** *360*, 112705.

(74) Deng, X.; Deng, M.; Li, Y.-L.; Liu, Z.; Liu, T.-F.; Chen, X.; Cai, S.; Liu, B.; Li, J.; Lv, D.; Li, J.; Yuan, W., A zinc-octacarboxylate MOF with an unusual (6, 8)-connected ocu topology for high-capacity adsorptive separation of C8 alkylaromatics. *Chem. Eng. J.* **2023,** *474*, 145694.

(75) Bae, H. J.; Kim, S.-I.; Choi, Y.; Kim, K.-M.; Bae, Y.-S., High p-xylene selectivity in aluminum-based metal–organic framework with 1-D channels. *J. Ind. Eng. Chem.* **2023,** *117*, 333-341.

(76) Yang, L.; Liu, H.; Yuan, D.; Xing, J.; Xu, Y.; Liu, Z., Efficient Separation of Xylene Isomers by a Pillar-Layer Metal–Organic Framework. *ACS Appl. Mater. Interfaces* **2021,** *13* (35), 41600-41608.

For Table of Contents Only